

Optical and Acoustic Characterisation of multimodal contrast agents for colorectal cancer lymph node detection

Georgia Adam¹, Vladimir Denisov², Zahra Rattray³, Adrian Thomson⁴, Susan Moug⁵, ²Tomas Jansson, Susan Farrington⁶, Carmel Moran⁴, Helen Mulvana¹

¹Department of Biomedical Engineering, University of Strathclyde, Glasgow, UK; ²Biomedical Engineering, Department of Clinical Sciences, Lund University, Lund, Sweden; ³Strathclyde Institute of Pharmacy & Biological Sciences, University of Strathclyde, Glasgow, UK; ⁴Centre for Cardiovascular Science, University of Edinburgh, UK; ⁵Department of Surgery, Royal Alexandra Hospital, UK; ⁶Cancer Research UK Edinburgh Centre, Institute of Genetics and Cancer, University of Edinburgh, UK;

BACKGROUND

Localisation of lymph nodes in colorectal cancer is integral to staging, surgical planning and patient outcomes [1]. However current clinical approaches (MRI, CT, lymphangiography) lack spatial resolution, sensitivity or are not well suited to the operating theatre. We propose magnetic ultrasound contrast agents for combined contrast-enhanced and magneto-motive ultrasound imaging (CE-MMUS) and present detailed characterisation of these novel contrast agents.

INTRODUCTION



Fig 1. MAGNETIC NPs

- Not echoic
- **Lymphatic agent** - aggregates in tissues and lymph nodes (MR contrast agent)

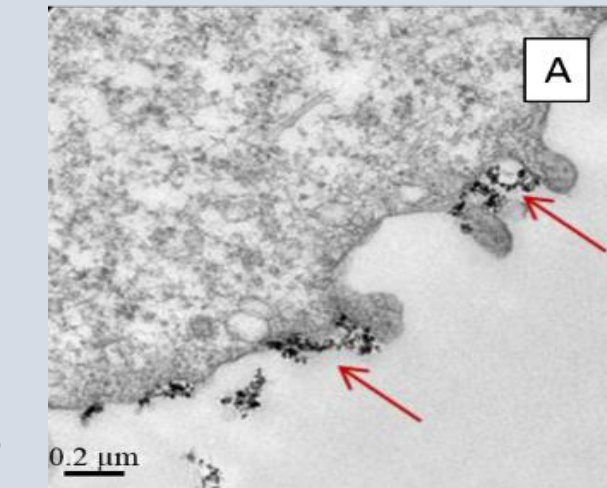


Fig 2. MICROBUBBLES

- Highly echoic
- Perfusion agent
- **Blood pool agent** – enables perfusion imaging (contrast enhanced ultrasound, CEUS)

RATIONALE

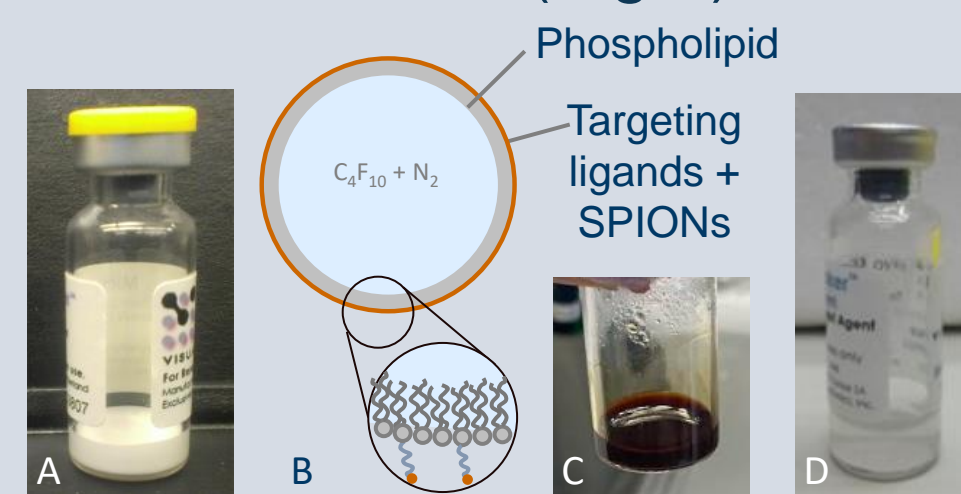
Magneto-motive ultrasound imaging (MMUS) uses an external magnetic field to displace super paramagnetic iron oxide nanoparticles (SPIONs) aggregated to lymph nodes [2]. Ultrasound imaging recovers the displacement for lymph node delineation. We aim to develop CE-MMUS using magnetic microbubbles (SPION-MBs) that we hypothesise will deliver enhanced tissue displacement [3], and may be combined with CEUS, as per prior work with standard pre-clinical contrast [4]. Pilot data indicates low concentrations of SPION-MBs aggregate to the lymph nodes, impairing utility for CE-MMUS. Nanoscale phase-change agents may offer a viable alternative.

AIM: Establish size, concentration, magnetic loading and acoustic behaviour of novel contrast agents suspensions for lymph node imaging

CONTRAST AGENT PREPARATION

Target ready micromarker (TR-MM, Fujifilm Visualsonics), a pre-clinical ultrasound contrast agent with streptavidin incorporated to the lipid shell, was reconstituted as per manufacturer's instructions to produce 700mL of suspension (2×10^9 bubbles/mL), SPIONs were biotinylated [5] (12.5mg/ml) and 42 μ L added to produce SPION-MBs. Efficacy of biotinylation was determined with fluorescence methods. Alternatively, TR-MM was condensed to produce nanodroplets [6], and SPIONs added to create SPION-NDs (Fig 3).

Fig 3: A TR-MM; B SPIONs-B + TR-MM schematic; C SPIONs; D condensed TR-MM



PARTICLE SIZING

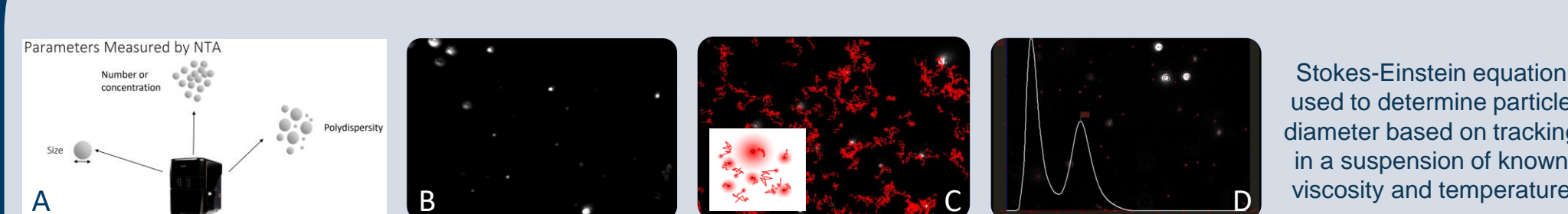


Fig 4. Nanoparticle tracking analysis (Nanosight, NS300, A) was used to image (B) and track particles in suspension (C & inset), to determine concentration, polydispersity and mean particle size (D) for each suspension

MAGNETIC LOADING

Mean SPIONs-B loading per TR-MM microbubbles was calculated through titration and ¹H Nuclear Magnetic Resonance.

ADV

Acoustic droplet vaporisation (ADV) of nanodroplet suspensions diluted 5:1 were established through scattering [7]. Suspensions flowed at 20 μ L/sec through the co-axial focus of 1 MHz HIFU transducer driven with 5 cycle sinusoid, 10 ms pulse repetition and passive cavitation detector. Scattered signals were acquired for post-processing in MATLAB

TISSUE MIMICKING MATERIALS

Polyacrylimide samples incorporating SPIONs or SPION-MBs were subject to MMUS / CE-MMUS to assess performance

Fig 5. MMUS schematic [2]

RESULTS

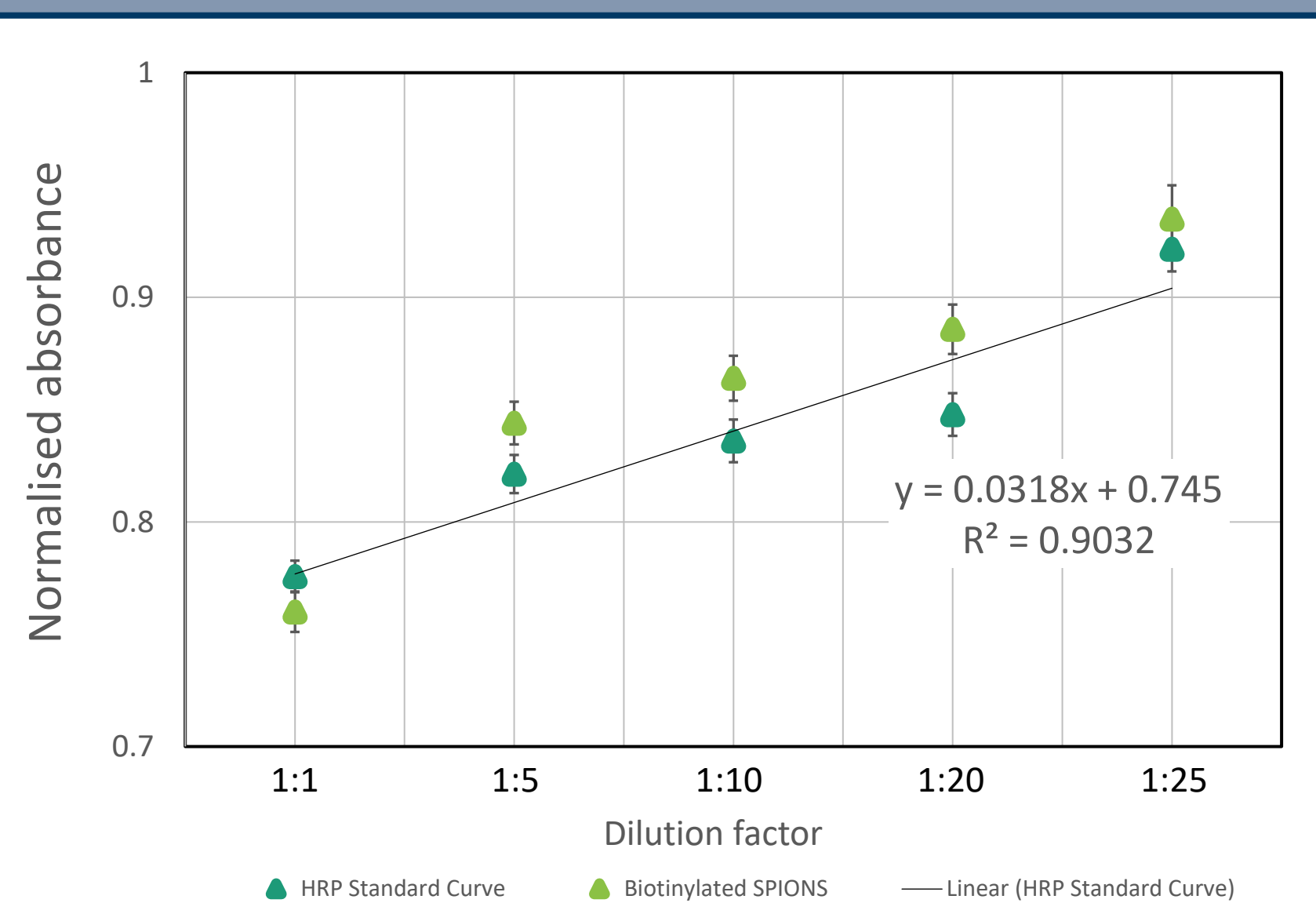


Fig 6. Three samples: SPIONs, SPIONs-B and HRP (control) were serially diluted and absorbance measured confirming successful biotinylation of SPIONs

Particle	Diameter (nm) [mean \pm st dev]
SPIONs	53.8 \pm 1.5
SPIONs-B	66.9 \pm 1.5
TR-MM	1100.0 \pm 180.0
TR-MM + SPIONs-B	138.0 \pm 166.0
Condensed TR-MM	129.2 \pm 5.1
Condensed TR-MM + SPIONs-B	138.6 \pm 44.2

Table 1: Suspension characterisation measured through NTA. Data indicate that SPIONs were successfully conjugated to TR-MM by streptavidin – biotin linkage. Minimal free SPIONs were measured in these suspension, confirming that >90% of SPIONs became conjugated to microbubbles. Condensation to produce droplets resulted in nanosized particles that retained their conjugation properties to load to SPIONs-B

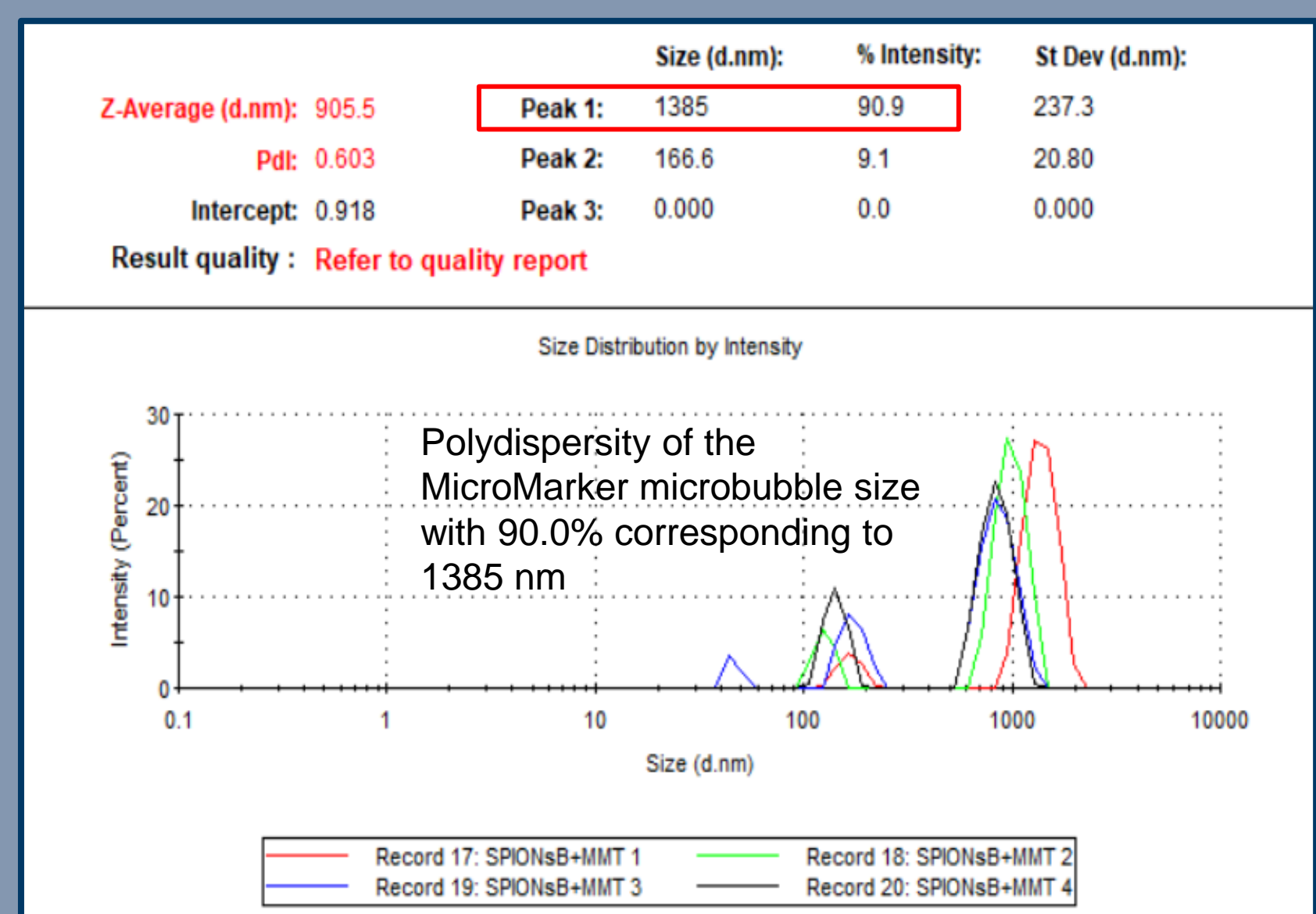


Fig 7. Size distribution by intensity, example NTA output, 90.9% of the particles have a diameter of 1.385 micrometers indicating the bond between SPIONs-B and TR-MM has taken place (<5% particles with diameter equal to SPIONs-B are present)

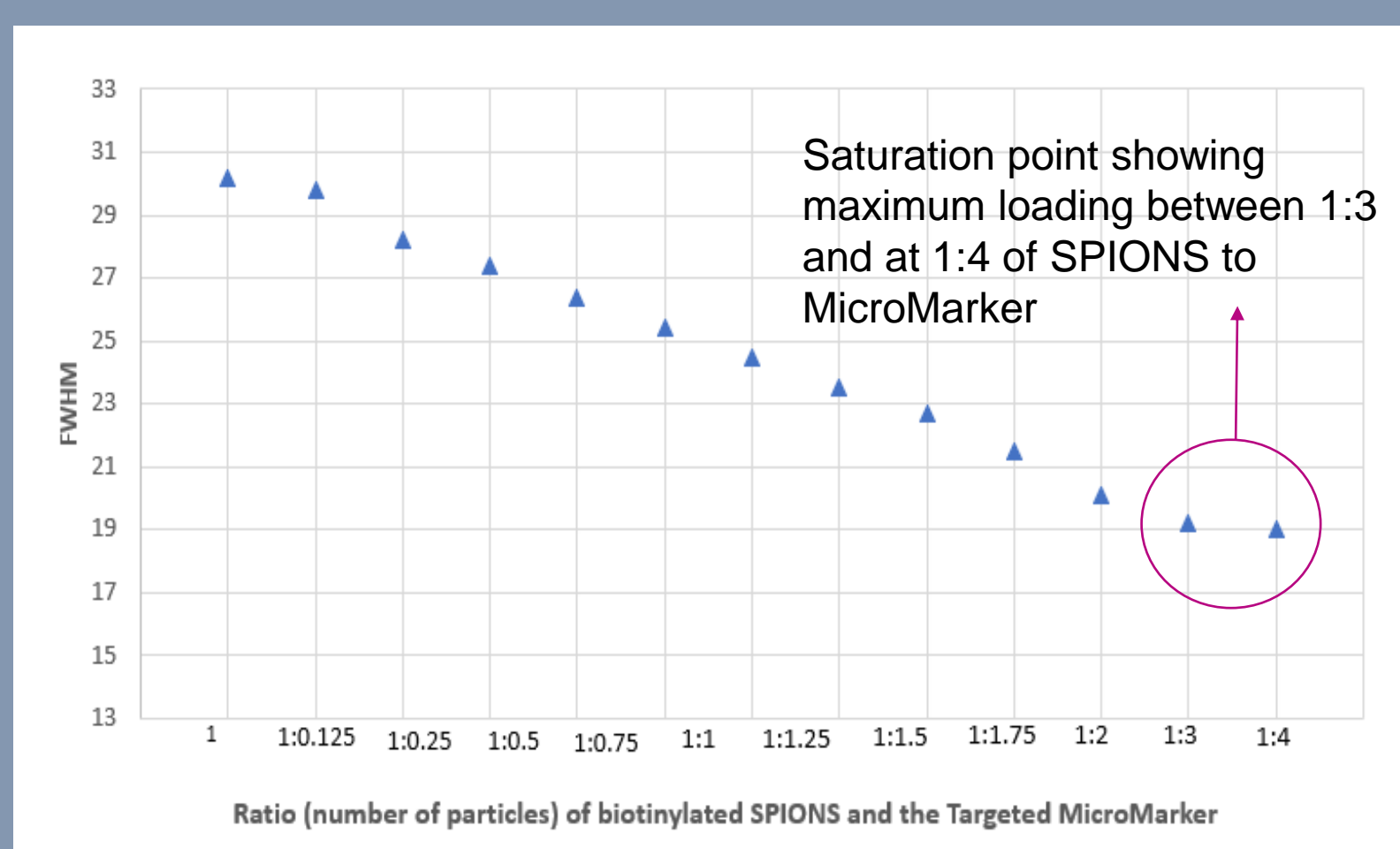


Fig 8. ¹H NMR measurement of suspensions with increasing SPIONs-B to TR-MM ratio were used to determine maximum loading of SPIONs that could be achieved per microbubble. Plot shows the Full Width Half Maximum (FWHM) measurement of the proton peak for each dilution ratio investigated. Data showed a gradual narrowing of the proton peak to the point that saturation occurs at a ratio of 1:3, indicating SPIONs-B have less surface area exposed to water due to complete binding to TR-MM

ADV...

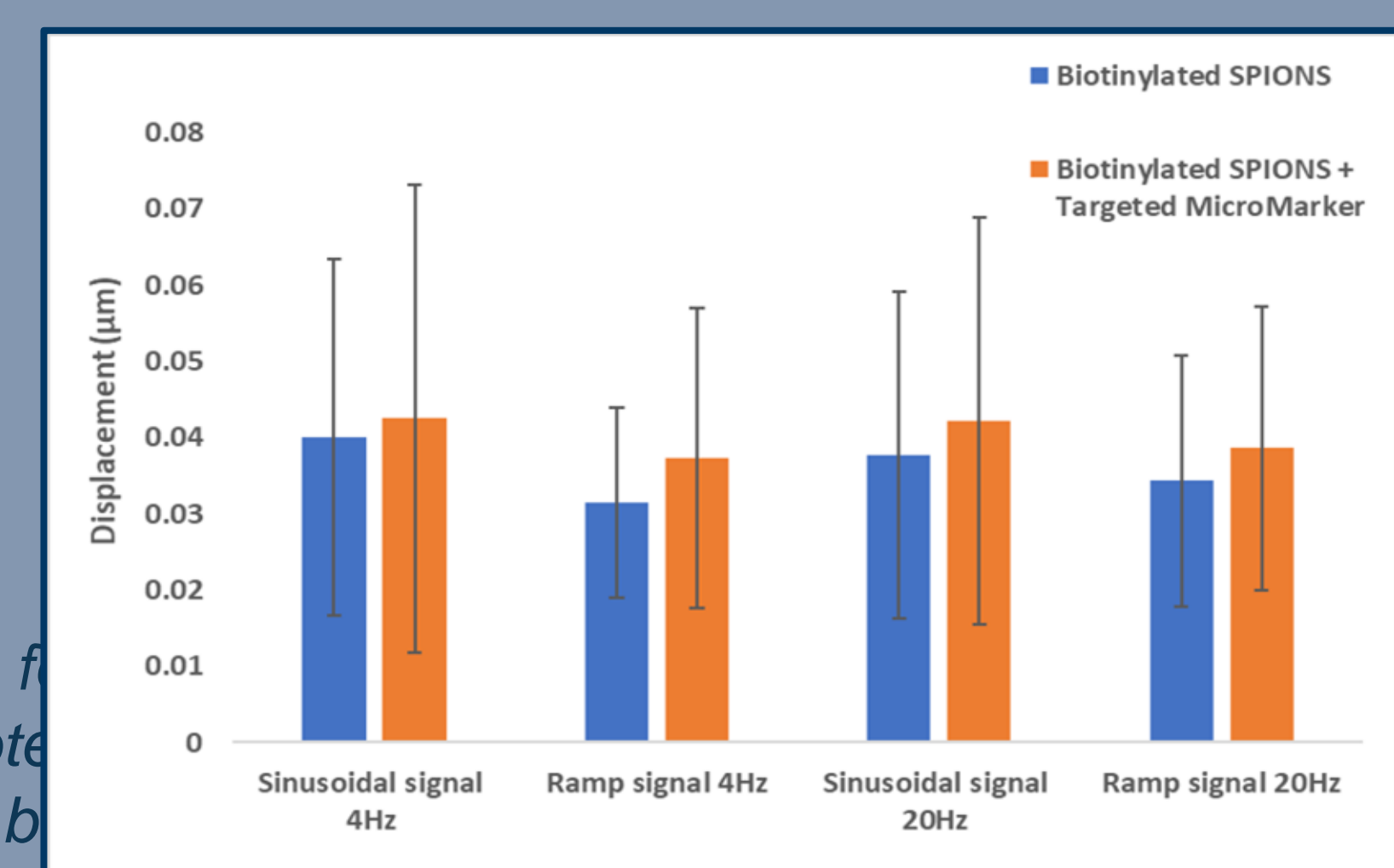


Fig 9. Preliminary data showing magneto-motive displacement values for PAAm containing either SPIONs-B or SPIONs-B + TR-MM. It can be noted that SPIONs-B + TR-MM display a trend towards higher displacement work continues to optimise experiments and confirm.

CONCLUSIONS

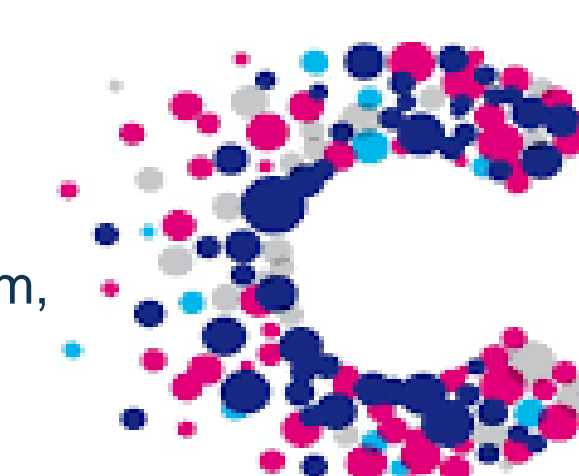
- Fluorescence methods confirmed biotin assay and establish SPION biotinylation.
- NTA measurements provide suspension sizing and concentration data, also confirming successful conjugation of SPIONs-B to TR-MM.
- ¹H NMR measurements determined maximum SPIONs-MM loading through titration.
- Polyacrylamide tissue mimicking materials containing SPIONs-B & SPIONs-B+MM will allow comparison of CE-MMUS performance through rms tissue displacement achievable

REFERENCES

- [1] ML Ong, JB Schofield, World J Gastrointest Surg 27; 8(3): 179-92, 2016
- [2] S Sjöstrand *et al* Ultras Med Biol 46(10): 2636-2650, 2021
- [3] S Sjöstrand *et al* Brit J Radiol 95(1135): 20211128, 2022
- [4] M Bacou *et al* Cancers, 14(3): 561, 2022
- [5] E Beguin *et al* Appl Mater Interfaces 11: 1829-1840, 2019
- [6] PS Sheeran *et al* Ultras Med Biol 43(2): 531-540, 2017
- [7] R Domingo-Roca *et al* IEEE International Ultrasonics Symposium, 2021

ACKNOWLEDGEMENTS

CRUK A2333 & 24730



CANCER RESEARCH UK